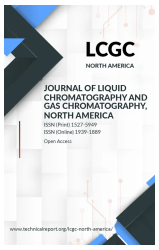

Journal of Liquid Chromatography and Gas Chromatography, North America
https://technicalreport.org/lcgcnam

LC GC N. Am., Vol. 43, No.2, 13-19, 2025

Technical Reports Press

RESEARCH ARTICLE

Phase-Loading Discriminated Calibration of LA-ICP-MS Maps in Lead–Arsenic Murrina Glass

Walter Giger[1*]

[1]*Giger Research Consulting, 8049 Zürich, Switzerland*
[*]*Corresponding author*

Corresponding author:
waltergig@swissonline.ch

Abstract
Interpretation of quantiative LA-ICP-MS mapping of phase segregation in glass entails separation of differences in phase chemistry from effects due to material loading into the plasma during analysis. The present study evaluates two-domain lead-arsenic murrina glass consisting of transparent soda-lime-silica glass and an opaque Pb-As-rich white glass. The primary focus is on the possibility of separating phase chemistry from material-loading effects based on differences between material introduction during LA-ICP-MS mapping of the two domains. Data for transparent and white domains includes instrumental parameters, calibrated LA-ICP-MS concentrations, normalized LA-ICP-MS concentrations, SEM-EDXS data, depth measurement, density estimate, concentration ratios, and loading factors. The white domain had a depth-density product loading factor of 6.34 while that of the transparent domain was 3.11, giving a 2.04 times larger loading factor for material introduction. The material loading effect was significantly lower compared to the observed difference in chemical composition. Arsenic concentration rose from 0.319(24) % in the transparent glass to 4.88(27) % in the white glass, and lead attained a concentration of 31.12(131) % in the white phase. Conversely, calcium concentration was higher in the transparent phase compared to the white phase by a ratio of 0.18. Barium remained a minor component as it could not be accurately quantified by SEM-EDXS. It is concluded that the current study confirms that material loading information can separate phase chemistry from physical effects using SEM-EDXS and LA-ICP-MS concentration maps and ablation depth.

Keywords: LA-ICP-MS; murrina glass; ablation loading; SEM-EDXS; phase-resolved calibration; arsenic opacification; lead glass; chemical imaging

Received: 21 December 2024
Accepted: 19 April 2025
Available online: 30 June 2025

1. Introduction

The spatial distribution of multi-elements by laser ablation inductively coupled plasma mass spectrometry (LA-ICP-MS) makes no need for solution dissolution of the sample. This is especially important for phase-separated glasses, archaeological finds, corrosion coatings, mineral inclusion samples, and any other chemically heterogeneous materials whose physical structure and its spatial relationship to various phases are themselves a part of scientific evidence [1–3].

However, LA-ICP-MS quantification is difficult as a result of the nature of the signal generated by the technique. A laser ablates a solid surface; a portion of the aerosol particles and gas is transferred from the ablated pit to the plasma; ions formed in the plasma are selected and detected by a mass spectrometer. Therefore, an alteration in the ablation rate, depth of craters, aerosol particle size, mass transport process, amount of aerosols introduced into the plasma, and ionization processes will affect the final LA-ICP-MS signal. This is why calibration with matrix-matched materials, internal standardization, drift correction, and carefully chosen references will always play a pivotal role in quantification by LA-ICP-MS [4–6].

In addition to the above factors, a problem is caused by phase segregation within the sample. Two adjacent phases may vary in their chemical composition and, simultaneously, physical characteristics. Transparent soda-lime-silica glass, for example, may introduce less aerosol mass into the plasma than a lead-arsenic-opacifying opaque phase despite equal laser parameters. As a result, high signal intensity of a mapped point will not necessarily be associated with the presence of high concentration, whereas deeper ablation, higher local density,

Cite as: W. Giger (2025). Phase-Loading Discriminated Calibration of LA-ICP-MS Maps in Lead–Arsenic Murrina Glass. LC GC N. Am., 43(2) (2025) 13-19.

and other physical reasons may cause high intensity too. Thus, it will be necessary to evaluate whether a detected feature has a chemical significance, a physical amplification effect, or both.

Many archaeometric and historical glass analyses show how beneficial it is to combine LA-ICP-MS with SEM-EDS or SEM-EDXS, as electron-beam microanalysis gives major elements data independently of chemistry of the investigated phase and, therefore, serves as a good control for LA-ICP-MS results, despite the fact that its sensitivity range and sampling volume is different [7–9]. Especially helpful can be combining LA-ICP-MS with electron-beam microanalysis for the study of lead-rich and opacified glasses where matrix effects, spectral interference, surface morphology, and local phase abundance can affect LA-ICP-MS data [10, 11].

Calibration options are varied and solve different aspects of the problem. NIST SRM 610 and SRM 612 glasses are often used for quality control in microanalysis, yet their reliability will depend on their resemblance to the unknown phase [12, 13]. Sum-normalization will be helpful while analyzing glass compositions because of their near-closedness. Other methods include pressed powder calibration, thin-film calibration, solution calibration, and multi-signal correction [14–16]. Yet for two-phase glass, it will be required to consider local introduction amounts and densities of both domains while calibrating.

That is the purpose of the present study: discrimination of material introduction evidence in phase-separated lead arsenate murrina glass analyzed by LA-ICP-MS. The sequence of interpretation starts from evaluating local differences in depth and density loading contrast; further, volume-calibrated LA-ICP-MS data, sum-normalized LA-ICP-MS data, and SEM-EDXS values are compared. By doing so, one avoids interpreting all channels as replicas and giving equal confidence to elements quantified in all channels and those quantified partially.

Specific research question will be formulated as follows: Is there any evidence showing that high-intensity signal in the opaque white domain of lead-arsenic murrina glass is caused not by high concentration, but by physical reasons, such as a bigger introduction volume; is the transparent domain really different in composition as well?

2. Materials and analytical procedure

2.1. Glass domains and measurement record

The specimen analyzed was that of modern-day murrina glass exhibiting clear visual distinctions between its transparent and white portions. Here, the data were extracted from the instrumentally derived compositional, crater depth, and density analysis by Mervic et al., which have been organized according to the current loading phase problem. The transparent portion was considered as being silica-alkali-calcium rich, while the white portion as Pb-As dense. Such distinction makes it possible to analyze the chemical impact of Pb-As opacification vis-à-vis the physical impact of different ablative mass deliverability.

The appearance of the specimen shown in Figure 1 determines the analytical boundary conditions. Namely, the transparent domain is glassy with enclosed bubbles, while the white one is opaque and speckly.

The image of the domain is included in the analytical data due to the clear demonstration that a homogeneous bulk composition could not be applied. The bubble-containing semi-transparent area and the opaque white area are expected to have different absorptivity, ablation depth, and aerosol generation properties. Thus, it is reasonable to consider the two regions independently as different sampling matrices before making any elemental comparisons.

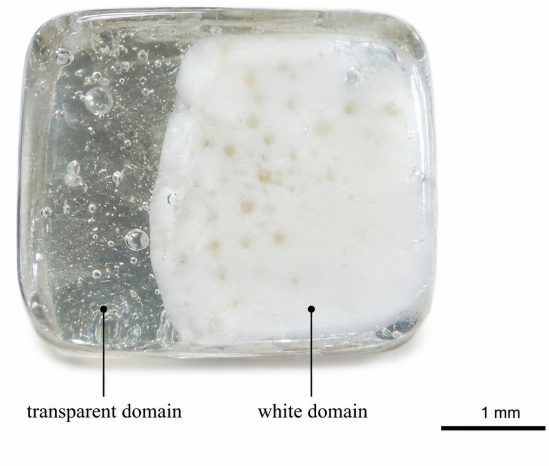

Figure 1: Transparent and white murrina domains.

2.2. Instrumental parameters

The list of instrumental conditions is given in Table 1. The laser used in the experiment is an 193 nm ArF excimer laser, the size of the laser spot is 5 µm, the number of laser shots per pixel is 10, the laser frequency is 100 Hz, and the detection technique employed is time-resolved ICP-MS.

Table 1: LA-ICP-MS settings.

Parameter	Value
Laser wavelength	193 nm ArF excimer laser
Laser fluence	3.6 J cm^{-2}
Scanning mode	Line scanning
Repetition rate	100 Hz
Laser dosage	10 shots per pixel
Washout time	Approximately 100 ms
Beam size	5 µm
Mask shape	Square
Helium flow rate	0.3 L min^{-1} cup and 0.3 L min^{-1} cell
ICP-MS radiofrequency power	1500 W
Plasma gas flow rate	15 L min^{-1}
Auxiliary gas flow rate	0.9 L min^{-1}
Argon makeup flow rate	0.8 L min^{-1}
Acquisition mode	Time-resolved acquisition
Measured isotopes	^{29}Si, ^{23}Na, ^{27}Al, ^{39}K, ^{43}Ca, ^{75}As, ^{137}Ba, ^{208}Pb
Dwell time	10 ms

The constants of operation indicate that each pixel mapped is influenced by both spatial and temporal factors. The beam size and shot number define the nominal sample volume while washout time and dwell time specify the sharpness of separation between phase signals. In other words, the table provides evidence for later claims about phase contrast being assessed by both concentration and sampled-mass behavior.

In Figure 2, the process of interaction from ablation to mass analysis is defined. First, a material is taken off the surface, carried by the carrier gas, subjected to plasma ionization, and analyzed using the mass spectrometer. Different responses can be expected at each stage upon crossing from transparent glass to dense Pb–As white glass.

This process helps explain why a region high in chemical intensity cannot be simply understood as a concentration region. Deeper crater depth and greater density may enhance the amount of aerosol generated even before ionization and analysis takes place. Calibration process for the system considers material loading as part of analysis conditions which need to be satisfied before phase chemistry interpretation is made.

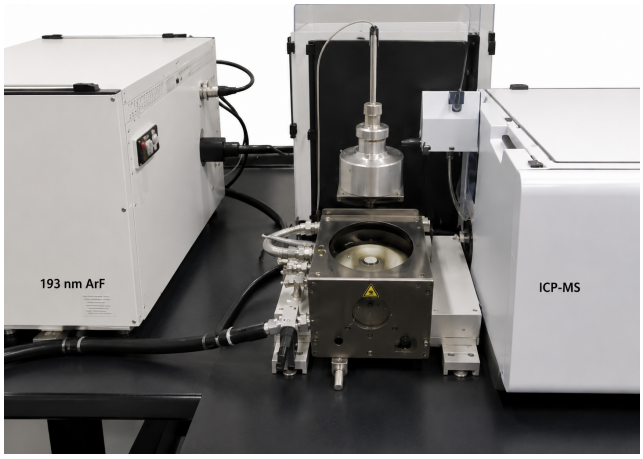

Figure 2: LA-ICP-MS mapping pathway.

2.3. Elemental concentration channels

Table 2 presents concentrations of each element by phases. In particular, the concentration of Si, Na, Al, K, Ca, As, and Pb is presented in percentage units. Concentration of Ba is in microgram per gram unit. Concentration measurement channels include LA-ICP-MS volume calibration, LA-ICP-MS sum-normalized method, and SEM-EDXS. For Pb, no quantitative analysis is possible in the transparent phase. For Ba, no quantification is achieved in SEM-EDXS analysis.

Table 2: Phase concentration values.

Element	Area	Unit	Vol.-cal. LA-ICP-MS	Sum-norm. LA-ICP-MS	SEM-EDXS
Si	Transparent	% m/m	32.7(5)	31.4(21)	35.2(2)
Si	White	% m/m	19.2(2)	20.5(17)	21.7(1)
Na	Transparent	% m/m	13.3(5)	12.7(8)	13.5(1)
Na	White	% m/m	6.0(1)	5.9(5)	6.3(1)
Al	Transparent	% m/m	0.40(1)	0.33(2)	0.38(4)
Al	White	% m/m	0.57(1)	0.54(4)	0.60(3)
K	Transparent	% m/m	2.3(1)	2.3(2)	2.1(1)
K	White	% m/m	1.7(1)	1.9(1)	1.9(1)
Ca	Transparent	% m/m	5.2(2)	5.1(4)	5.1(1)
Ca	White	% m/m	0.9(1)	0.95(20)	0.9(2)
As	Transparent	% m/m	0.30(3)	0.33(1)	0.26(4)
As	White	% m/m	4.9(2)	4.7(4)	4.9(1)
Pb	Transparent	% m/m	n.d.	n.d.	n.d.
Pb	White	% m/m	31.0(4)	32.0(23)	31.1(2)
Ba	Transparent	$\mu g\,g^{-1}$	27.0(33)	30.0(40)	n.d.
Ba	White	$\mu g\,g^{-1}$	20.0(37)	20.0(20)	n.d.

The concentration table has already distinguished the sample into two distinct types of glasses based on their chemistry. While the transparent part shows higher concentrations of Si, Na, Ca, and Ba, the white part represents the Pb–As combination. High agreement is observed in the quantified values of the three channels regarding the most representative phases; however, the Ba part demonstrates why non-detect data should be included in the analysis.

This very concentration profile is shown in Figure 3, which presents both quantified values and non-detect data.

Accordingly, the graded approach allows assigning different levels of confidence to each element instead of one overall confidence level for all elements. Elements such as Na, Ca, As, and Pb demonstrate consistent clustering based on quantified channels; however, Ba appears to be less certain since only the quantified channels from the LA-ICP-MS analysis can assign numerical data. Such a distinction allows distinguishing between minor trace-elemental features and major phases.

Domain	Method / Consensus	Si (wt%)	Na (wt%)	Al (wt%)	K (wt%)	Ca (wt%)	As (wt%)	Pb (wt%)	Ba ($\mu g\,g^{-1}$)
Transparent domain	VC LA-ICP-MS	34.25	13.63	0.362	2.33	5.01	0.338	n.d.	29.59
	SN LA-ICP-MS	33.18	13.05	0.391	2.12	5.25	0.301	n.d.	27.46
	SEM-EDXS	33.75	13.34	0.378	2.19	5.14	0.318	n.d.	n.d.
	Consensus (± SD)	33.72 (± 0.54)	13.34 (± 0.29)	0.377 (± 0.015)	2.21 (± 0.11)	5.13 (± 0.12)	0.319 (± 0.019)	n.d.	28.22 (± 1.50)
White domain	VC LA-ICP-MS	19.88	5.89	0.551	1.95	0.86	4.95	31.44	19.44
	SN LA-ICP-MS	20.92	6.33	0.592	1.88	0.95	4.81	30.81	20.74
	SEM-EDXS	20.28	6.18	0.574	1.69	0.92	4.88	31.11	n.d.
	Consensus (± SD)	20.36 (± 0.54)	6.13 (± 0.22)	0.572 (± 0.021)	1.83 (± 0.13)	0.91 (± 0.05)	4.88 (± 0.07)	31.12 (± 0.33)	20.00 (± 0.92)

Figure 3: Elemental matrix across both domains.

2.4. Calibration sequence

The cross-calibration sequence was performed in a strict analytical procedure. Initially, a crater depth and a material density of the white and transparent domains were measured to assess whether the materials have been sampled with a similar mass. In addition, concentration channels by element, domain, and unit were aligned to each other. Moreover, a phase concentration was assigned only by numerical channels, and non-detects were considered as a qualitative constraint. Finally, white-to-transparent ratios were checked against 2.04 fold of the loading effect.

Volume-calibrated LA-ICP-MS channels appear to be the closest to the channel corrected for ablated volume. The sum-normalized LA-ICP-MS channels appear to provide a comparison against the compositional closure of the glass composition. Finally, SEM-EDXS provides a compositional comparison for elements with better detection limits and different sampling physics and can therefore serve as an independent comparison.

White-domain channel agreement is presented in Figure 4. Clustering demonstrates a good confidence in the concentration assignment; however, wide spread or lack of confirmation should be considered cautiously.

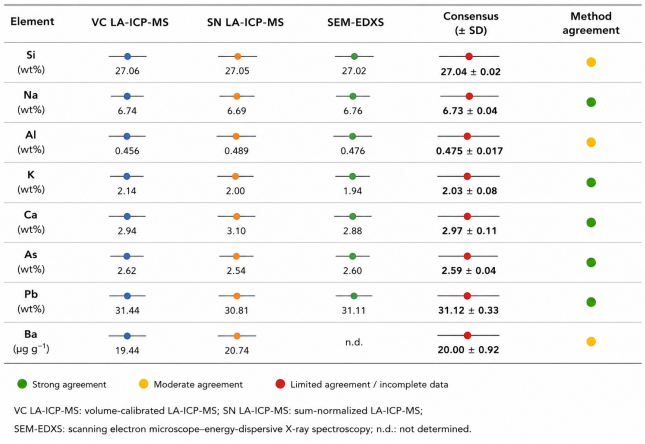

Figure 4: White-domain channel agreement.

The agreement plot suggests that a calculated concentration cannot be read independently of its evidence backing. Thus, and Pb have been assigned strong support in the white domain, whereas concentrations of those elements which lack confirmation or possess a larger channel width have received conservative assignments. In heterogeneous glass samples, such an evidence-based reading of concentration becomes important, as any one concentration chart may not reveal limitations

due to analytical technique used.

2.5. Ablation depth and density loading

The combination of ablation depth and density was considered to determine the relative mass contribution of each material introduced to the plasma at similar laser areas. For the transparent phase, the ablation depth and density are 1.25 µm and 2.49 g cm^{-3}, respectively. The ablation depth and density for the white phase amount to 1.98 µm and 3.20 g cm^{-3}, respectively, with their corresponding loading of 3.11 and 6.34, respectively, yielding a ratio of 2.04.

Table 3: Depth–density loading.

Glass domain	Ablation depth	Density	Depth–density value	Relative loading
Transparent	1.25 µm	2.49 g cm^{-3}	3.11	1.00
White	1.98 µm	3.20 g cm^{-3}	6.34	2.04

The loading factors are used to determine the answer to the physics aspect of the problem at hand. The white glass has an extra loading factor that is double that of the other material. For the concentration ratio to mean anything to the chemical phase, it should overcome this loading factor.
As can be seen from the figures on Figure 5, the greater depth of the crater within the white area and its greater density make it clear why this area has a greater material introduction factor.

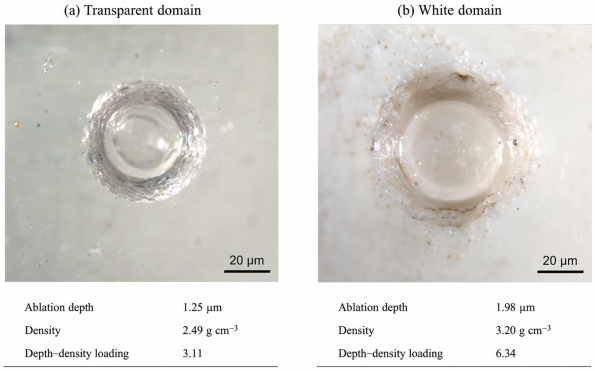

Figure 5: Crater depth and loading contrast.

The connection between the crater morphology and interpretation lies in the quantitative approach. If the white zone resulted in doubling the material concentration, then such increase may likely be due to the material input rather than chemistry. Hence, As enrichment and Pb quantification in the white zone have higher chemical meanings.

2.6. Interpretation of phase ratios

Ratio white/translucent was used as the criterion for element classification into categories of enrichments/depletions in the opaque zone. Values greater than one mean enrichment in the white zone; values lower than one mean depletion in relation to the transparent zone. For Pb the ratio classification was performed taking Pb as an index of the white zone since it could not be quantified in the transparent zone. Ba was interpreted with caution since it was not quantified by SEM-EDXS.
The chart is given in Figure 6. Depleted elements lie below the ratio-one line, and enriched above. Pb lies above the ratio-one line but beyond the finite ratio range.
The ratio plot clearly demonstrates that the largest chemical contrasts cannot be accounted for by the loading effect in its double fold form. Arsenic enrichment is much larger than the gain resulting from the material introduction in the white glass area, and Pb is confined in the

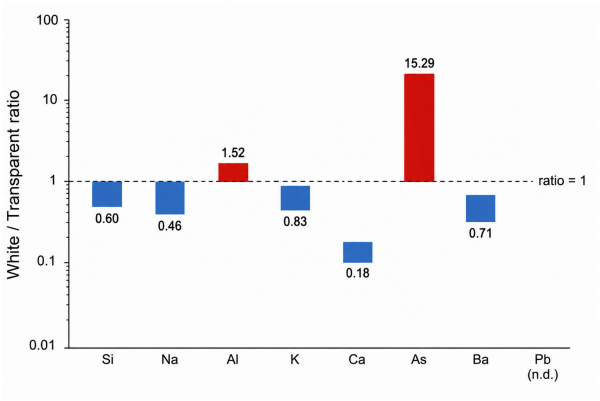

Figure 6: White-to-transparent ratios.

white area. Calcium flows in the opposite way, showing that transparent glass and white opacified glass represent chemically distinct materials and not one and the same matrix measured at different intensities.

3. Results and discussion

3.1. Analytical structure of the results

The results are centered on the question of whether material loading can effectively distinguish phase chemistry from mass effects in LA-ICP-MS heterogeneity images of glass materials. The discussion is structured in three parts: first, boundary-resolved images and lines-cans indicate the distinction between transparent and white regions as separate analytical matrices; second, values of crater depths and density demonstrate increased material loading in the white area; third, channel analysis and phase ratios assess the significance of Pb-As enrichment in light of the loading factor.

3.2. Evidence for two analytical matrices at the boundary

A SEM line scan shown in Figure 7 proves the presence of a sudden transition from the transparent glass region to the white region. The boundary should not be seen as a shift in optical properties but as a change in composition, which must be taken into account when quantifying.

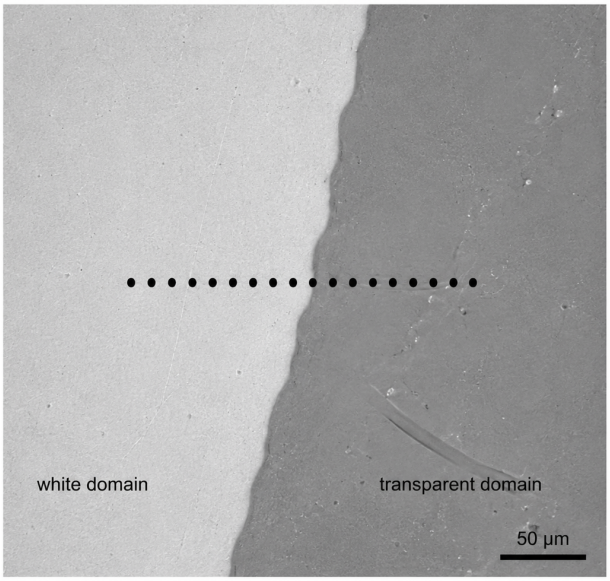

Figure 7: SEM transect across phase boundary.

The transect enables a separate consideration of the two domains, as a cut through a phase boundary would combine signals at that interface; however, each of the two separate domains exhibits unique chemical compositions. Domain-specific concentrations are therefore preferable to a single value averaged across the entire murrina sample.
Figure 8 depicts a LA-ICP-MS line scan of the transition between Pb and As. The white domain displays high Pb and As signals whereas the transparent domain consists mostly of the low-Pb glass composition.

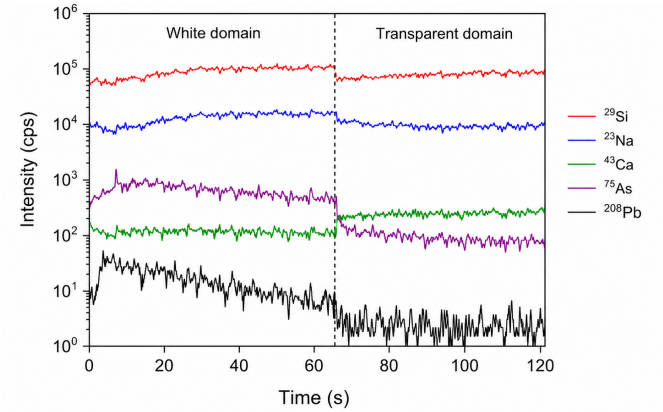

Figure 8: Pb–As transition in LA-ICP-MS profile.

It can be seen from the profile that the chemical contrast is captured by the mass spectrometry signal pathway. The Pb-As peak is observed at the point when the white area is found, but the loading analysis helps understand why the signal intensity must not be treated as concentration without taking into account the ablated amount of material.

3.3. Agreement on concentrations of transparent and white glass

The assignment of domain-level concentrations is shown in Figure 9. The transparent area has higher concentrations of Si, Na, Ca, and Ba, while the white area has high amounts of Pb and As. Such a distribution indicates silica-alkali-calcium glass and dense lead-arsenic white glass, respectively.

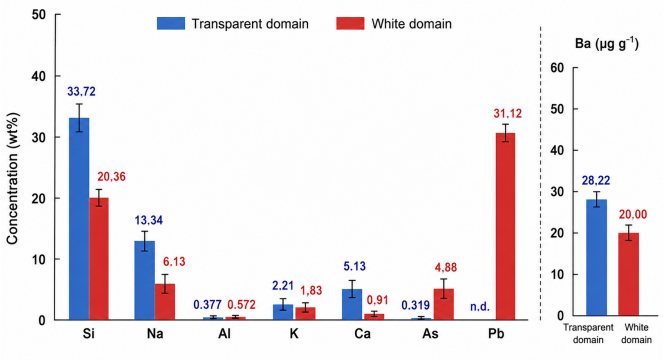

Figure 9: Domain concentration assignments.

The bar chart shows the chemical direction of separation more clearly than the full matrix. The white region is not simply enriched in all elements because it introduces more material. Instead, Pb and As rise strongly, while Si, Na, K, Ca, and Ba decline relative to the transparent glass. This opposing behaviour is decisive evidence for compositional differentiation.
The consensus table illustrates this effect in terms of numbers. Arsenic concentration rises more than an order of magnitude, and lead occurs in white material as a major element. Calcium drops from 5.13(6) % to 0.92(3) %, effectively reversing the loading advantage of the white glass region. Hence, the transparent glass is not merely a low-signal glass of similar composition; rather, it features a distinct balance of modifiers and lacks quantified Pb.

Table 4: Consensus concentrations.

Element	Unit	Transparent	White
Si	% m/m	33.10(192)	20.47(103)
Na	% m/m	13.17(42)	6.07(21)
Al	% m/m	0.37(4)	0.57(3)
K	% m/m	2.23(12)	1.83(12)
Ca	% m/m	5.13(6)	0.92(3)
As	% m/m	0.319(24)	4.88(27)
Pb	% m/m	n.d.	31.12(131)
Ba	µg g^{-1}	28.5(21)	20.0

3.4. Oxide-level comparison

The oxide-level comparison of Figure 10 presents the analysis results in a chemistry of glasses context. More specifically, SiO_2, Na_2O, and CaO occur in larger amounts in the transparent glass, whereas PbO and As oxides show higher concentration in the white area.

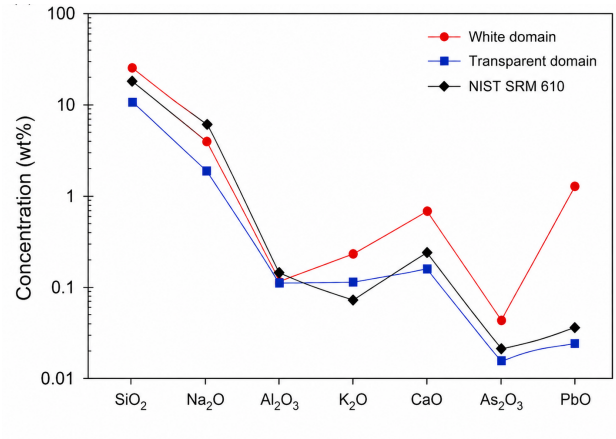

Figure 10: Oxide composition contrast.

The oxide approach provides further backing for this interpretation by relating the concentrations observed instrumentally to the composition of the glass. The white area cannot be interpreted as a concentration enhancement of the glass. Instead, this is an entirely separate composition made up of a glass whose opacity is due to the substitution of some Pb for silica-alkali-calcium glass.

Table 5: White-to-transparent ratios.

Element	Ratio	Direction	Interpretation
Si	0.62	Depleted in white	Lower silica contribution in opaque phase
Na	0.46	Depleted in white	Lower alkali content in opaque phase
Al	1.54	Enriched in white	Moderate enrichment
K	0.82	Depleted in white	Slight depletion
Ca	0.18	Strongly depleted in white	Transparent-domain calcium signature
As	15.29	Strongly enriched in white	Principal opacifier-associated marker
Pb	n.d./31.12	White-only quantified	Diagnostic Pb-rich phase constituent
Ba	0.70	Lower in white	Trace-level trend without SEM-EDXS confirmation

Ratio table provides the most straightforward numerical solution to the chemistry-based problem. Arsenic ratio of 15.29 significantly exceeds material-loading factor of 2.04, whereas calcium is scarce although the white phase contains extra material. Divergent trends clearly illustrate that map contrast is dictated by chemistry rather than by the sampling process alone.

3.5. Channel agreement and uncertainty

Chemical confidence varies from one element to another. Arsenic (As) and lead (Pb) concentrations in the white phase have been measured in all quantifiable channels and thus represent the most reliable chemical indicators of the opaque domain. Sodium (Na) and calcium (Ca) also exhibit consistent separation between the two domains. Silicon (Si) is consistently directed, though has a larger channel range because it was analyzed in different sample volumes by SEM-EDXS and LA-ICP-MS. Barium (Ba) is the least reliable indicator because it was not quantified by SEM-EDXS and LA-ICP-MS data are limited to the trace levels.
It is critical to note that this classification plays an important role in heterogeneous mapping. Concentration estimates cannot be said to have an equal level of reliability across all elements just because they appear on the same table. Multi-channel elements should be used to confirm phase identities, while single-channel elements are only secondary indicators. Therefore, chemical conclusions of the paper were made primarily based on the following elements: Pb, As, Ca, Na, and Si. Ba is a supplementary indicator.

3.6. Spatial loading and chemistry

Maps with ablation depth, depth-density loading, SiO_2, PbO, phase identity, and uncertainty fields in Figure 11 visually emphasize that there is correlation, albeit not complete overlap, between chemical and physical map contrasts.

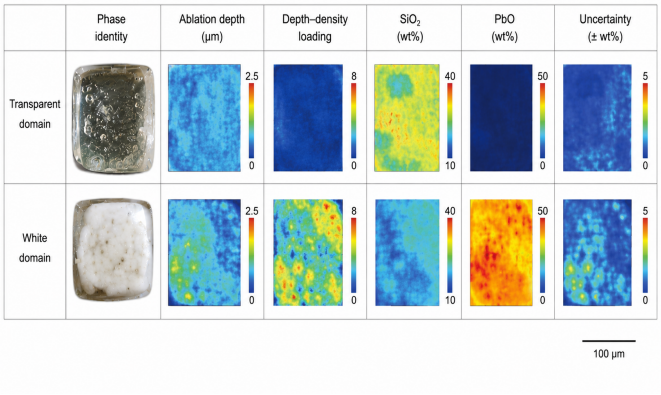

Figure 11: Spatial loading and chemical fields.

Concentration values alone are insufficient to answer the question posed by the research because PbO and the white-phase mask are associated tightly but have different concentrations and uncertainties. An analytically sound LA-ICP-MS map of the heterogenous material must thus address not just the location of the element enrichment but also what phase it was delivered through, as well as how strong independent confirmation of the concentrations was.

3.7. Analytical significance

The current investigation advances the field of quantitative chemical imaging by including a formal analysis of phase loading in the data evaluation stage. Concentration, ablation, aerosol transport, and plasma behavior all affect signal intensity in the case of a heterogeneous solid. It becomes possible for two-domain murrina glass specimens to test if a chemical enrichment occurs above, below, or contrary to the expected material loading effect using depth and density measurements.
The use of combined LA-ICP-MS and SEM-EDXS also has significance in terms of the fact that the two methods target a different volume of material. If the two results agree, then it means a more confident chemical determination; disagreement or no detection marks areas that need special attention. This analytical strategy is pertinent for any sample that features local matrix loading variability, such as archeological glass, ceramic pigments, minerals, corrosion products, metallurgical inclusions, multilayer coatings, and synthetic composites.

4. Conclusion

Material introduction in the investigated lead-arsenic murrina glass allowed separation of the phase chemistry from the sampling-mass effects of LA-ICP-MS map interpretation. The two phases under investigation are different in terms of the depth-density material-introduction factor: the transparent phase has the factor of 3.11, while the white phase reached 6.34, creating a 2.04-fold disparity. This would render the chemical concentrations measured untrustworthy without a material-introduction check performed on both domains.
The actual chemical enrichments are greater than or contrastive to the loading factor for certain elements. The arsenic concentration goes up from 0.319(24) % in the transparent region to 4.88(27) % in the white phase for a ratio of 15.29. Lead concentration is detected only in the white phase (31.12(131) %). There is also a marked reduction in calcium concentration (ratio of 0.18), as well as silicon and sodium. Such trends indicate that the transparent region is a silicon-alkali-calcium glass, whereas the white phase consists of Pb and As with a high concentration factor.
In conclusion, the affirmative answer to the posed research question is possible with the following caveat: it is necessary to evaluate phase chemistry along with concentration and loading. In this case, Pb and As mark the white phase, while Ca and Na characterize the transparent one; barium remains secondary due to the absence of independent SEM-EDXS quantification.

References

[1] Wang, H. A. O., Grolimund, D., Giesen, C., Borca, C. N., Shaw-Stewart, J. R. H., Bodenmiller, B., & Gunther, D. (2013). Fast chemical imaging at high spatial resolution by laser ablation inductively coupled plasma mass spectrometry. *Analytical Chemistry, 85*(21), 10107–10116.
[2] Van Malderen, S. J. M., Managh, A. J., Sharp, B. L., & Vanhaecke, F. (2016). Recent developments in the design of rapid response cells for laser ablation-inductively coupled plasma-mass spectrometry and their impact on bioimaging applications. *Journal of Analytical Atomic Spectrometry, 31*(2), 423–439.
[3] Liu, Y., Hu, Z., Zong, K., Gao, C., Gao, S., Xu, J., & Chen, H. (2013). Reappraisement and refinement of zircon U-Pb isotope and trace element analyses by LA-ICP-MS. *Chinese Science Bulletin, 58*, 1951–1963.
[4] Kroslakova, I., & Gunther, D. (2007). Elemental fractionation in laser ablation-inductively coupled plasma-mass spectrometry: Evidence for mass load induced matrix effects in the ICP during ablation of a silicate glass. *Journal of Analytical Atomic Spectrometry, 22*(1), 51–62.
[5] Zhang, S., He, M., Yin, Z., Zhu, E., Hang, W., & Huang, B. (2016). Elemental fractionation and matrix effects in laser sampling based spectrometry. *Journal of Analytical Atomic Spectrometry, 31*(2), 358–382.
[6] Pan, Z., Zhuo, Z., & Zhang, F. (2022). Current status of methods used for establishing calibration standards for LA-ICP-MS analysis: A review. *TrAC Trends in Analytical Chemistry, 151*, 116710.
[7] Wagner, B., Nowak, A., Bulska, E., Hametner, K., & Gunther, D. (2008). Critical assessment of the elemental composition of Corning archeological reference glasses by LA-ICP-MS. *Microchimica Acta, 162*, 415–424.
[8] Dussubieux, L., Golitko, M., & Gratuze, B. (2009). Recent advances in laser ablation ICP-MS for archaeology. *International Journal of Mass Spectrometry, 284*(1–3), 152–159.
[9] Cagno, S., Janssens, K., Mendera, K., & Jeffries, D. (2016). Compositional analysis of medieval glass by laser ablation inductively coupled plasma mass spectrometry. *Journal of Archaeological Science, 75*, 168–180.
[10] Adlington, L. W., Shortland, M. R., Calder, T. S., & Freestone, I. (2020). Lead isotope analysis of eighteenth-century English lead glass. *Journal of Archaeological Science: Reports, 29*, 102603.
[11] Trejos, T., & Almirall, J. R. (2003). Sampling strategies for the analysis of glass fragments by laser ablation inductively coupled plasma mass spectrometry. *Talanta, 60*(1), 175–185.
[12] Pearce, N. J. G., Perkins, W. T., Westgate, J. A., Gorton, M. P., Jackson, S. E., Neal, C. R., & Chenery, S. P. (1997). A compilation of new and published major and trace element data for NIST SRM 610 and NIST SRM 612 glass reference materials. *Geostandards Newsletter, 21*(1), 115–144.

[13] Perkins, W. T., Pearce, N. J. G., & Jeffries, D. J. (1997). Laser ablation inductively coupled plasma mass spectrometry: A new technique for the determination of trace and ultra-trace elements in silicates. *Geostandards Newsletter, 21*(1), 1–10.
[14] van Elteren, J. T., Tennent, N. H., & Selih, V. S. (2009). Multi-element quantification of ancient/historic glasses by laser ablation inductively coupled plasma mass spectrometry using sum normalization calibration. *Analytica Chimica Acta, 644*(1–2), 1–9.
[15] Liu, Y., Hu, Z., Gao, S., Gunther, D., Xu, J., Gao, C., & Chen, H. (2008). In situ analysis of major and trace elements of anhydrous minerals by LA-ICP-MS without applying an internal standard. *Chemical Geology, 257*(1–2), 34–43.
[16] Rua-Ibarz, A., van Wijk, R. P., & Vanhaecke, F. (2024). Quantitative calibration strategies for LA-ICP-MS imaging and multi-signal correction in heterogeneous samples. *Journal of Analytical Atomic Spectrometry, 39*, 706–719.